Title

Bioelectronic neuromodulation of the paravertebral cardiac efferent sympathetic outflow and its effect on ventricular electrical indices

Journal

Heart Rhythm, 14(7)

ISSN

1547-5271

Authors

Buckley, Una
Chui, Ray W
Rajendran, Pradeep S
et al.

Publication Date

2017-07-01

DOI

10.1016/j.hrthm.2017.02.020

Peer reviewed

HHS Public Access

Author manuscript

Heart Rhythm. Author manuscript; available in PMC 2017 July 01.

Published in final edited form as:

Heart Rhythm. 2017 July ; 14(7): 1063–1070. doi:10.1016/j.hrthm.2017.02.020.

Bioelectronic neuromodulation of the paravertebral cardiac efferent sympathetic outflow and its effect on ventricular electrical indices

Una Buckley, MD[1,2,*], **Ray W. Chui, MS**[1,2,3,*], **Pradeep S. Rajendran, BS**[1,2,3], **Tina Vrabec, PhD**[4], **Kalyanam Shivkumar, MD, PhD**[1,2,3], and **Jeffrey L. Ardell, PhD**[1,2,3]

[1]University of California – Los Angeles (UCLA) Cardiac Arrhythmia Center, David Geffen School of Medicine, Los Angeles, CA, USA

[2]UCLA Neurocardiology Research Center of Excellence, David Geffen School of Medicine, Los Angeles, CA, USA

[3]Molecular, Cellular & Integrative Physiology Program, UCLA, Los Angeles, CA, USA

[4]Department of Biomedical Engineering, Case Western Reserve University, Cleveland, OH, USA

Abstract

Introduction—Neuromodulation of the paravertebral ganglia, using symmetric voltage controlled kilohertz frequency alternating current (KHFAC), has the potential to be a reversible alternative to surgical intervention in patients with refractory ventricular arrhythmias. KHFAC creates scalable focal inhibition of action potential conduction.

Objective—To evaluate the efficacy of KHFAC, when applied to T1–T2 paravertebral chain, to mitigate sympathetic outflow to the heart.

Methods—In anesthetized, vagotomized, porcine subjects the heart was exposed via midline sternotomy along with paravertebral chain ganglia. The T3 paravertebral ganglion was electrically stimulated and activation recovery intervals (ARI) were obtained from a 56-electrode sock placed over both ventricles. A bipolar Ag electrode was wrapped around the paravertebral chain between T1 and T2 and connected to a symmetric, voltage controlled KHFAC generator. Comparison of cardiac indices during T3 stimulation conditions, with and without KHFAC, provided a measure of block efficacy.

Corresponding Author: Jeffrey L. Ardell, Ph.D., UCLA Neurocardiology Research Center of Excellence, UCLA Cardiac Arrhythmia Center, UCLA Health System, 47-126 CHS, Los Angeles, CA 90095, 310-825-0417, jardell@mednet.ucla.edu.

* These authors contributed equally.

competing interests: Authors report no conflict of interest with respect to these studies.

Author contributions: *Authors UB and RWC contributed equally to the design, execution and data analysis of study. PSR, TV contributed in experiments and in technology development. KS and JLA contributed to conceptual design and analytics. UB drafted the manuscript. All authors edited the manuscript. All authors approved the final version of the manuscript.

Results—Right-sided T3 stimulation (4Hz) was titrated to produce reproducible ARI changes from baseline (52±30ms). KHFAC resulted in a 67% mitigation of T3 electrical stimulation effects on ARI (18.5±22ms, $p<0.005$). T3 stimulation repeated after KHFAC produced equivalent ARI changes as control. KHFAC evoked a transient functional sympatho-excitation at onset that was inversely related to frequency and directly related to intensity. Optimum block threshold was 15 kHz and 15 volts.

Conclusions—KHFAC applied to nexus (convergence) points of the cardiac nervous system produce a graded and reversible block of underlying axons. As such, KHFAC has the therapeutic potential for on-demand and reversible mitigation of sympatho-excitation.

Introduction

Sudden cardiac death, as a result of ventricular arrhythmias, is often the first presenting sign of structural heart disease [1]. Autonomic dysregulation secondary to cardiac pathology is central to the development of heart failure and ventricular arrhythmias [2, 3]. Surgical removal of the T1–T4 paravertebral chain reduces ventricular arrhythmia burden, by removing excessive sympathetic input to the cardiac myocytes [4, 5]. Although effective, by decentralizing peripheral cardiac sympathetic control from the central nervous system, surgically removing a section of the sympathetic paravertebral ganglia (T1–T4) evoked off-target side effects including thoracic hyperalgesia and/or compensatory abdominal hyperhidrosis in patients [4].

In managing transient episodic autonomic imbalances, an alternative way of targeting the cardiac nervous system would be technologies that allow for on-demand suppression of cardiac sympathetic activity in a reversible manner. This can be accomplished through a bioelectronic therapy called axonal modulation therapy (AMT). One iteration of AMT is symmetric, voltage controlled kilohertz frequency alternating current (KHFAC) [6]. This technology uses electrical current to directly inhibit the local conduction of action potentials [6]. KHFAC, as applied to somatic nerves, produces rapid block of nerve conduction that is quickly reversible [6, 7]. However, one confounding effect with KHFAC is that an onset response, reflective of excitation before block, accompanies current initiation [6, 7]. The utility of KHFAC to dynamically manage cardiac control via the autonomic nervous system has not been evaluated.

Sympathetic control of the heart reflects the dynamic interplay between central and intrathoracic aspects of the cardiac nervous system [2, 3, 8]. To control sympathetic outflow to the heart it is critical to target primary nexus (convergence) points where pre and/or post-ganglionic projections run together prior to their divergence to atrial and ventricular tissues via branches of the thoracic vagosympathetic nerve trunk; the T1–T2 segment of the paravertebral chain is a nexus point for sympathetic control of the heart [9, 10]. By surgically removing T1–T2 we are able to block sympathetic efferent control of ventricular activation recovery intervals [9]. The upper thoracic aspects of the paravertebral chain are readily accessible in pigs and man [5, 11, 12]; well suited as future targets for chronic AMT.

The primary objective of this study was to evaluate the efficacy of KHFAC, when applied to T1–T2 paravertebral chain, to mitigate sympathetic outflow to the heart in a reversible

manner. By reversibly inhibiting the nerve conduction in the paravertebral chain, one could scale the level of sympathetic efferent inputs to the heart, limit the potential for off target effects (as in the case of surgical decentralization [4]) and can switch back on full cardiac sympathetic control as required.

Methods

The study protocol was approved by the University of California Los Angeles Institutional Animal Care and Use Committee and conforms to the National Institutes of Health Guide for the Care and Use of Laboratory Animals (Eight Edition, 2011).

Surgical preparation

Yorkshire pigs (n=12) were sedated with tiletamine-zolazepam (4–8mg/kg, intramuscular) and anesthetized with isoflurane (1–5%, INH). After endotracheal insertion the animals were ventilated and general anaesthesia was maintained with inhaled isoflurane (1–2%) and boluses of fentanyl (20–30ug/kg, intravenous (IV)) as required during surgery. The depth of anesthesia was assessed throughout the experiments by monitoring corneal reflexes, jaw tone, and hemodynamic indices. Once the surgical preparation was completed, the anaesthesia was switched to α-chloralose bolus (50mg/kg over 30 minutes, titrated based on hemodynamic response and depth of anesthesia) and subsequent maintenance infusion (20–35mg/kg/hr IV). The femoral artery and vein were cannulated for monitoring of systemic pressure and infusion of fluids or medications respectively. A posterior 12 lead electrocardiogram was placed and end tidal carbon dioxide monitoring maintained between 35–45mmHg. Arterial blood gas sampling was assessed on a 1–2 hourly basis and adjustments to tidal volume, respiratory rate or doses of sodium bicarbonate performed to maintain adequate oxygenation and homeostasis.

A midline sternotomy was performed to expose the heart and paravertebral sympathetic ganglia from T1–T4. The cervical vagi were isolated and transected bilaterally (n=9). In a subset of animals (n=3), paravertebral stimulation and KHFAC were applied in animals with intact vagi and with pre-treatment with atropine (1mg/kg). After the surgical preparation there was a 1 hour stabilization period. On completion of the experiment, the animals were euthanized by administration of sodium pentobarbital (100mg/kg, iv) with potassium chloride (1–2mEq/Kg, iv) under high dose isoflurane (5% inhaled).

Hemodynamic measurements

A 5 French Millar pressure catheter (SPR-350) was inserted into the left ventricle via the left carotid artery. This was connected to the MVPS Ultra Pressure Volume Loop System (Millar Instruments, Houston, Texas). From this measurement of left ventricular (LV) pressure, cardiac contractility (dP/dt), and heart rate were derived. A lead II ECG, LV pressure and system pressure were input to a Cambridge Electronics Design (model 1401) data acquisition system for continuous monitoring of hemodynamic status.

Activation recovery index recording and analysis

A custom made 56-electrode epicardial sock was placed over both ventricles to provide regional unipolar electrograms for the ventricular epicardium. This data was collected via a Prucka CardioLab system (GE Healthcare, Fairfield, CT) and analysed using customized software (ScalDyn M, University of Utah, Salt Lake City, UT). ARI was assessed similarly to previous published work by our group [9, 13]. In brief, the activation time was measured from the beginning of the first derivative of the derived voltage (dV/dt) in the depolarization wave of the intrinsic deflection of voltage. The recovery time was the maximum dV/dt to time of the peak of repolarization (T wave). The ARI is the recovery time minus the activation time. ARI has been shown to correlate with regional ventricular action potential duration [14].

Sympathetic electrical stimulations of the stellate and T3 paravertebral ganglion

The stellate and T3 paravertebral ganglia were stimulated using bipolar needle electrodes with and without KHFAC. The bipolar electrodes were interfaced with Grass S88 stimulators (Grass Co., Warwick, RI) via SIU6 constant current stimulus isolation units. Electrical stimulation of the stellate and T3 ganglia were titrated at 4Hz to achieve a 10% increase in left ventricular end systolic pressure, heart rate, dP/dt max or decrease in activation recovery interval (ARI). After threshold was identified, the stimulus intensity used thereafter was 1.5 times threshold, applied for 30 second periods. Between sequential nerve stimulations there was a waiting period of 10 minutes to allow for all parameters to return to baseline.

KHFAC

A bipolar Ag electrode was placed around the paravertebral sympathetic axons between T1 and T2 (figure 1). This electrode interface was then connected to a charge-balanced, voltage controlled, square wave, KHFAC waveform function generator (Stanford Research System, Sunnyvale, CA) with varying frequency and voltages assessed from 5–20 kHz and 5–20 Volts. A capacitor was placed in series on each output line of the waveform generator to prevent direct current contamination of the signal. A symmetric KHFAC implies a zero net charge.

Protocol for assessing block induced by KHFAC

Baseline ventricular epicardial ARI, LV contractility (dP/dt), and heart rate were assessed. They were then evaluated with (T1) stellate ganglion and T3 stimulations with and without KHFAC. T3 electrical stimulation was performed 10 min after each KHFAC to ensure complete recovery of nerve function. During KHFAC T1 stimulation was performed to assess whether KHFAC had an effect on nerve conduction proximal to the electrode. Between stimuli there was a waiting period of ten minutes to ensure complete recovery of hemodynamic and electrical indices to baseline. KHFAC stimulation resulted in a transient activation of the sympathetic nervous system prior to blocking nerve conduction. Therefore, there was a waiting period of at least two minutes or until the hemodynamic and electrical indices return to baseline parameters before blocking efficacy was assessed by T3 stimulation. If after 5 minutes of KHFAC the cardiac hemodynamic indices did not return to

baseline then KHFAC was discontinued and frequency or intensity re-adjusted to mitigate the onset response.

Protocol for assessing the onset response to KHFAC

Baseline ventricular epicardial activation recovery intervals, LV contractility, and heart rate were assessed. KHFAC was applied 15 seconds and the change in hemodynamic and electrical indices from baseline assessed. The range of frequencies and voltages tested was from 5 to 20 kHz and 5–20 volts. At least 5 min separated sequential KHFAC challenges.

Statistical analysis

Statistical analysis was done using Sigma Stat (SigmaStat Software, San Jose, CA) with one-way repeated ANOVA of variance for comparing hemodynamic and regional ventricular indices with and without KHFAC. Paired Student t test and Wilcoxon rank sum were also performed for comparison of continuous variables. Data was considered statistically significant where the $P<0.05$. Data are presented as a mean ± SE.

Results

KHFAC block assessment

Chronotropic, dromotropic and inotropic responses to baseline stimulations —In 9 porcine subjects (5 male, 4 female), weighing on average 41±3kg, paravertebral KHFAC applications were assessed. T1 (stellate) and T3 stimulations were titrated to produce equivalent changes in heart rate and ventricular ARI. At 4Hz, stimulation parameters of 2.2±0.3mA for RT1, 3.3±0.8mA for RT3, 3.2±0.9mA LT1, and 9.3±5.7mA LT3 produced at least a 10% increase in LVSP, heart rate or shortening of ARI and were defined as threshold. Subsequent T1 and T3 stimulations were done at 4Hz, 1.5× threshold.

Baseline T3 stimulations resulted in a change in ARI on 51±15ms on the right sympathetic paravertebral ganglia and 26±10ms for the left ($p<0.05$). T3 stimulation also resulted in a heart rate change of (34±11bpm right; 6±8bpm left) and LVSP change of (22±5mmHg right; 22±7mmHg left). The maximum dP/dt was augmented with T3 stimulation by (657±38mmHg/s right; 689±176mmHg/s left). Repeated T3 stimulations resulted in a consistent response throughout the experiment.

Chronotropic, dromotropic and inotropic responses to KHFAC—Figure 2 shows a representative cardiac hemodynamic onset response to initiation of KHFAC, the blunted cardiac response to subsequent RT3 stimulation when delivered during KHFAC and the full reversibility of this block in the recovery phase (RT3 Post). Note that the efficacy of block was manifest for heart rate, LV dp/dt and LV pressure. Note also that at 15 kHz and 15 volts KHFAC the onset response had extinguished within 1 minute of initiation.

Figure 3 shows a polar map indicating regional ventricular ARI in response to RT3 stimulation prior to and during KHFAC (15 kHz, 15 volts). The pattern of ARI shortening evoked at the onset of KHFAC (panel D) paralleled that with RT3 stimulation (panel B), but rapidly returned towards but not all the way back to baseline control (panel E). The positive

dromotropic effect evoked by RT3 stimulation (panel B) was mitigated by KHFAC (panel F) with no aberrant conduction pathways evident.

Figure 4 summarizes the average evoked cardiac hemodynamic response to T3 stimulation prior to, during and following KHFAC (15±0.8 kHz, 15±1.3 volts). The evoked cardiac response to T3 stimulation repeated in the presence of KHFAC were significantly reduced for ventricular ARI (−14.8±2.8% vs −5.2±3.1%), heart rate (36.5±7% vs 11.0±5.1%), LV +dp/dt (57.7±18.7% vs 16.1±7.7%) and LVSP (20.2±3.0% vs 10.3±3.1%). Equivalent levels of cardiac hemodynamic responses were evoked prior to and following KHFAC; indicative of the reversible nature of short duration block imposed by high-frequency alternating current applied to the paravertebral chain. For example, percentage change in ARI pre (15±7%) and post (18 ±11%) KHFAC were evoked with right-sided T3 stimulation.

Figure 5 illustrates the cardiac hemodynamic response evoked in response to stellate ganglia (RT1) stimulation prior to and in the presence of KHFAC. This stimulation point is upstream from the block location and demonstrates the focal nature of the current blocking at the T1–T2 level that does not interfere with ganglia processing capabilities of the stellate.

KHFAC onset response

KHFAC resulted in an onset response at the start of current delivery indicative of the initial activation phase evoked on underlying axons prior to establishment of blockade. Figure 2 shows a representative onset response to 15 kHz, 15 volt charge-balanced AC current. Onset responses varied with the characteristics of the stimulus waveform. In a separate subset of experiments (n=3), the onset response and blocking efficacy of KHFAC were maintained in animals with intact cervical vagi and with pre-emptive atropine (data not shown). Figure 6 illustrates the 3D response surfaces for the maximal onset response for heart rate (panel A), LV +dp/dt (panel B) and ventricular ARI (panel C) with the drive variable being frequency and intensity of KHFAC (n=9). Note that for all parameters, lower frequencies and higher intensities are associated with larger onset responses. This in turn is reflective of higher degrees of onset evoked sympatho-excitation. In the case of high level onset responses, often they had not extinguished by the end of the 5 min test period and T3 evaluations were aborted. The overall objective for KHFAC, or any form of AMT, is to optimize interfaces and stimulus protocols to minimize the onset response while maintaining flexibility to scale the degree of block during sustained current delivery.

Discussion

Neuromodulation utilizing bioelectronics methodologies have the potential to regulate nerve traffic and ganglionic processing within the cardiac nervous system. While KHFAC has been assessed in many peripheral nerve preparations [6, 7], this is the first proof-of-concept use of KHFAC on the cardiac sympathetic nervous system. The main conclusions from this paper are: i) KHFAC applied to the T1–T2 region of the paravertebral chain inhibits/modulates functional sympathetic efferent projections to the heart in a scalable and reversible manner; ii) An onset augmenting response precedes the axonal blocking during KHFAC; iii) the onset response can be mitigated by adjusting KHFAC parameters; and iv) KHFAC, when

deployed, can be activated on demand to counteract endogenous excessive sympatho-excitation.

Structure/function of the cardiac nervous system is a critical aspect for rational neuromodulation based therapy [2]. Control of cardiac function involves the dynamic interplay between neural networks contained on the heart (intrinsic cardiac ganglionated plexus), extracardiac intrathoracic ganglia, spinal cord, brainstem and higher centers of the central nervous system [2]. For sympathetic control, descending projections from the brainstem innervate preganglionic soma located in the intermediolateral cell column (C7–T4 spinal levels) [2, 15]. Preganglionic soma project axons via the paravertebral chain to post-ganglionic soma located in the stellate, middle cervical, mediastinal ganglia and intrinsic cardiac ganglia [2, 9, 10]. Each of these ganglia contains a complex network of afferent, efferent and local circuit neurons that interdependently work as a distributed neural network sub-serving cardio-cardiac reflexes [2]. Disruptions in reflex processing between central and peripheral aspects of the cardiac nervous system is a major contributing cause to arrhythmia formation [3, 16] and the progression of heart failure [17, 18]. Neuromodulation based therapies targeted to mitigate this central/peripheral imbalance are of obvious clinical importance.

Patients with intractable ventricular arrhythmias can be effectively treated with surgical procedures that include removing the paravertebral chain from T4 up to and including the lower third of the stellate ganglia [5]. While such surgical approaches have documented anti-arrhythmic effects [4, 5], these patients frequently experience off-target adverse effects including upper thoracic and limb hyperhidrosis and hyperalgesia [4]. We have recently demonstrated that cardiac-related preganglionic fibers arising from the thoracic cord traverse up the paravertebral chain through the T1–T2 region [9], some making synaptic contact with post-ganglionic neurons in the stellate with others projecting through the ansae subclavia to more distal intrathoracic ganglia (middle cervical, mediastinal and intrinsic) [19, 20]. As such, the ansae subclavia and the T1–T2 region of paravertebral chain are critical nexus points for sympathetic nerve traffic to and afferent projections from the heart [2, 9]. Based on structure/function considerations both sites are potential targets for axonal modulation therapy.

KHFAC has been applied to the cervical vagus, the sciatic nerve, the tibial and common peroneal nerve and the dorsal region of the thoracic spinal cord [6, 21, 22]. KHFAC refers to AC in the range of 1–100 KHz and without DC offset [6]. It is being used for a variety of pathological neural activity including limb and back pain management [21, 23]. High frequency bioelectronic nerve block mediates its effects by producing a reversible local conduction block [6]. The mechanism of conduction block is most likely via sodium channel inactivation [6]. Studies by Kilgore and others suggest that that KHFAC results in increased inward sodium current compared to the outward potassium current [24–26]. This depolarization resulted in activation of about 90% of the sodium channels in the node directly under the electrode [24]. Neurotransmitter depletion as opposed to true nerve conduction block [25] is not the mechanism as confirmed herein by a local conduction block at and distal to the KHFAC but not proximal to the KHFAC with stellate ganglion stimulation. As demonstrated in peripheral [6, 7] and now sympathetic nerves, the local conduction block reverses rapidly and can be applied multiple times without degradation in the underlying nerve processes.

Clinical Perspectives

Sudden cardiac death secondary to ventricular arrhythmias is a major clinical problem [27]. Cardiac pathologies such as ischemic heart disease disrupt the autonomic nervous system [1, 3, 8]. Ventricular electrical storm has been treated with medications [28], thoracic epidural anesthesia [5], and in the case of refractory ventricular arrhythmias surgical resection [4, 5, 29]. Surgical resection of the sympathetic paravertebral ganglia, while effective, results in adverse side-effects for patients [4]. Axonal modulation therapy poses a rapid and reversible way to target the sympathetic nervous system and thereby control the level of functional efferent input to the heart. Electrical currents applied to nerves at high frequency can directly inhibit conduction of action potentials [6, 7]. Based on anatomical considerations [9, 12], the preferred site for control of sympathetic input to heart in humans is to deploy the KHFAC electrodes to the T1–T2 region of the paravertebral chain, an area readily accessible by video-assisted thoracic surgery as routinely done for cardiac sympathetomy [5]. It should also be considered that the initial application of KHFAC results in a transient axonal activation termed the onset response [6, 7]. While the onset response can be mitigated by modifications in stimulation protocol and characteristics of the electrode/nerve interface such as contact size/spacing [6], future studies may involve development of hybrid technologies that include of KHFAC and DC current [30]. It can be envisioned that AMT can be implemented as part of an on-demand system to mitigate periods of central/peripheral imbalances in leading to sympatho-excitation.

Limitations

These experiments were done in anesthetized pig with no underlying pathology. They were also done with vagotomy to minimize confounding influences evoked from vagal afferents and efferents in reflex response to imposed stressors [31]. Blocking functional parasympathetic efferent effects with atropine in animals with intact vagi did not interfere with the onset or blocking response to T1–T2 paravertebral KHFAC. Future studies should consider the effects of neural remodelling in cardiac disease [32–34] on the efficacy of axonal modulation therapy. It should also be considered that T1–T2 region of the paravertebral chain as well as the ansae subclavia are mixed nerves containing both afferent and efferent projecting fibers [2]. While future studies should consider the potential contributions of afferent vs efferent control [35], it is clear from the current study that KHFAC of mixed sympathetic nerve does not evoke aberrant cardiac conduction, at least in normal animals. The transient axonal activation as a result of KHFAC, in the case of the sympathetic nervous system and the presence of structural heart disease, could potentially result in lethal ventricular arrhythmias if the onset response is not adequately controlled. The onset response may be mitigated by adjusting KHFAC parameters [6]. Finally, these studies only assessed the effects of relatively short-term KHFAC. Future studies should consider the effects (plasticity and memory) of longer-term and chronic KHFAC on integrated control of the cardiac nervous system.

Acknowledgments

Sources of funding

Work supported by contract from Glaxo-Smith-Kline (JLA, KS).

The authors acknowledge the inputs from Drs. Kevin Kilgore and Niloy Bhadra (Case Western Reserve University) in their review of the manuscript and in sharing their recognized experience in bioelectronic technologies of KHFAC nerve block. The authors acknowledge Dr. Arun Sridhar (Glaxo Smith Kline) in concept development.

References

1. Chugh SS, Reinier K, Teodorescu C, et al. Epidemiology of sudden cardiac death: clinical and research implications. Prog Cardiovasc Dis. 2008; 51:213–228. [PubMed: 19026856]
2. Ardell JL, Andresen MC, Armour JA, et al. Translational neurocardiology: preclinical models and cardioneural integrative aspects. J Physiol. 2016; 594:3877–3909. [PubMed: 27098459]
3. Fukuda K, Kanazawa H, Aizawa Y, Ardell JL, Shivkumar K. Cardiac innervation and sudden cardiac death. Circ Res. 2015; 116:2005–2019. [PubMed: 26044253]
4. Vaseghi M, Gima J, Kanaan C, et al. Cardiac sympathetic denervation in patients with refractory ventricular arrhythmias or electrical storm: intermediate and long-term follow-up. Heart Rhythm. 2014; 11:360–366. [PubMed: 24291775]
5. Bourke T, Vaseghi M, Michowitz Y, et al. Neuraxial modulation for refractory ventricular arrhythmias: value of thoracic epidural anesthesia and surgical left cardiac sympathetic denervation. Circulation. 2010; 121:2255–2262. [PubMed: 20479150]
6. Kilgore KL, Bhadra N. Reversible nerve conduction block using kilohertz frequency alternating current. Neuromodulation. 2014; 17:242–254. discussion 254–245. [PubMed: 23924075]
7. Bhadra N, Kilgore KL. High-frequency electrical conduction block of mammalian peripheral motor nerve. Muscle Nerve. 2005; 32:782–790. [PubMed: 16124008]
8. Shen MJ, Zipes DP. Role of the autonomic nervous system in modulating cardiac arrhythmias. Circ Res. 2014; 114:1004–1021. [PubMed: 24625726]
9. Buckley U, Yamakawa K, Takamiya T, Andrew Armour J, Shivkumar K, Ardell JL. Targeted stellate decentralization: Implications for sympathetic control of ventricular electrophysiology. Heart Rhythm. 2016; 13:282–288. [PubMed: 26282244]
10. Norris JE, Foreman RD, Wurster RK. Responses of the canine heart to stimulation of the first five ventral thoracic roots. Am J Physiol. 1974; 227:9–12. [PubMed: 4843349]
11. Arora RC, Waldmann M, Hopkins DA, Armour JA. Porcine intrinsic cardiac ganglia. Anat Rec A Discov Mol Cell Evol Biol. 2003; 271:249–258. [PubMed: 12552641]
12. Janes RD, Brandys JC, Hopkins DA, Johnstone DE, Murphy DA, Armour JA. Anatomy of human extrinsic cardiac nerves and ganglia. Am J Cardiol. 1986; 57:299–309. [PubMed: 3946219]
13. Vaseghi M, Zhou W, Shi J, et al. Sympathetic innervation of the anterior left ventricular wall by the right and left stellate ganglia. Heart Rhythm. 2012; 9:1303–1309. [PubMed: 22465457]
14. Haws CW, Lux RL. Correlation between in vivo transmembrane action potential durations and activation-recovery intervals from electrograms. Effects of interventions that alter repolarization time. Circulation. 1990; 81:281–288. [PubMed: 2297832]
15. Foreman, RDD., MJL, Linderoth, B. Integrative control of cardiac function by cervical and thoracic spinal neurons. In: Armour, JA., Ardell, JL., editors. Basic and Clinical Neurocardiology. New York: Oxford University Press; 2004. p. 153-186.
16. Kember G, Armour JA, Zamir M. Neural control hierarchy of the heart has not evolved to deal with myocardial ischemia. Physiol Genomics. 2013; 45:638–644. [PubMed: 23695889]
17. Florea VG, Cohn JN. The autonomic nervous system and heart failure. Circ Res. 2014; 114:1815–1826. [PubMed: 24855204]
18. Zucker IH, Patel KP, Schultz HD. Neurohumoral stimulation. Heart Fail Clin. 2012; 8:87–99. [PubMed: 22108729]
19. Beaumont E, Salavatian S, Southerland EM, et al. Network interactions within the canine intrinsic cardiac nervous system: implications for reflex control of regional cardiac function. J Physiol. 2013; 591:4515–4533. [PubMed: 23818689]
20. Armour JA. Potential clinical relevance of the ‘little brain’ on the mammalian heart. Exp Physiol. 2008; 93:165–176. [PubMed: 17981929]
21. Foreman RD, Linderoth B. Neural mechanisms of spinal cord stimulation. Int Rev Neurobiol. 2012; 107:87–119. [PubMed: 23206679]

22. Patel YA, Saxena T, Bellamkonda RV, Butera RJ. Kilohertz frequency nerve block enhances anti-inflammatory effects of vagus nerve stimulation. Sci Rep. 2017; 7:39810. [PubMed: 28054557]
23. Van Buyten JP, Al-Kaisy A, Smet I, Palmisani S, Smith T. High-frequency spinal cord stimulation for the treatment of chronic back pain patients: results of a prospective multicenter European clinical study. Neuromodulation. 2013; 16:59–65. discussion 65–56. [PubMed: 23199157]
24. Ackermann DM, Bhadra N, Gerges M, Thomas PJ. Dynamics and sensitivity analysis of high-frequency conduction block. J Neural Eng. 2011; 8:065007. [PubMed: 22056338]
25. Kilgore KL, Bhadra N. Nerve conduction block utilising high-frequency alternating current. Med Biol Eng Comput. 2004; 42:394–406. [PubMed: 15191086]
26. Bromm B. Spike frequency of the nodal membrane generated by high-frequency alternating current. Pflugers Arch. 1975; 353:1–19. [PubMed: 1079083]
27. Stecker EC, Reinier K, Marijon E, et al. Public health burden of sudden cardiac death in the United States. Circ Arrhythm Electrophysiol. 2014; 7:212–217. [PubMed: 24610738]
28. Priori SG, Blomstrom-Lundqvist C, Mazzanti A, et al. 2015 ESC Guidelines for the management of patients with ventricular arrhythmias and the prevention of sudden cardiac death: The Task Force for the Management of Patients with Ventricular Arrhythmias and the Prevention of Sudden Cardiac Death of the European Society of Cardiology (ESC). Endorsed by: Association for European Paediatric and Congenital Cardiology (AEPC). Eur Heart J. 2015; 36:2793–2867. [PubMed: 26320108]
29. Schwartz PJ. Cardiac sympathetic denervation to prevent life-threatening arrhythmias. Nat Rev Cardiol. 2014; 11:346–353. [PubMed: 24614115]
30. Franke M, Vrabec T, Wainright J, Bhadra N, Bhadra N, Kilgore K. Combined KHFAC + DC nerve block without onset or reduced nerve conductivity after block. J Neural Eng. 2014; 11:056012. [PubMed: 25115572]
31. Ardell JL, Rajendran PS, Nier HA, KenKnight BH, Armour JA. Central-peripheral neural network interactions evoked by vagus nerve stimulation: functional consequences on control of cardiac function. Am J Physiol Heart Circ Physiol. 2015; 309:H1740–1752. [PubMed: 26371171]
32. Ajijola OA, Yagishita D, Reddy NK, et al. Remodeling of stellate ganglion neurons after spatially targeted myocardial infarction: Neuropeptide and morphologic changes. Heart Rhythm. 2015; 12:1027–1035. [PubMed: 25640636]
33. Rajendran PS, Nakamura K, Ajijola OA, et al. Myocardial infarction induces structural and functional remodelling of the intrinsic cardiac nervous system. J Physiol. 2016; 594:321–341. [PubMed: 26572244]
34. Hardwick JC, Ryan SE, Beaumont E, Ardell JL, Southerland EM. Dynamic remodeling of the guinea pig intrinsic cardiac plexus induced by chronic myocardial infarction. Auton Neurosci. 2014; 181:4–12. [PubMed: 24220238]
35. Yamakawa K, Howard-Quijano K, Zhou W, et al. Central vs. peripheral neuraxial sympathetic control of porcine ventricular electrophysiology. Am J Physiol Regul Integr Comp Physiol. 2016; 310:R414–421. [PubMed: 26661096]

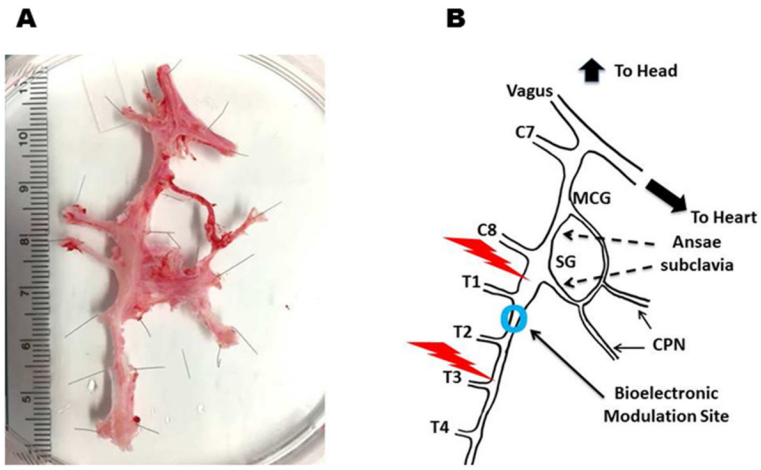

Figure 1.

Anatomy of the paravertebral sympathetic ganglia. Panel A: Dissected specimen from a porcine model showing the paravertebral chain (c7–T4), stellate ganglia (SG) and interconnections to middle cervical ganglia (MCG). Panel B: Stylized image demonstrates two nexus points for axonal modulation therapy for cardiac sympathetic control, the ansae subclavia and between T1–T2 of the paravertebral sympathetic ganglia. Stim, stimulation; CPN, cardiopulmonary nerve.

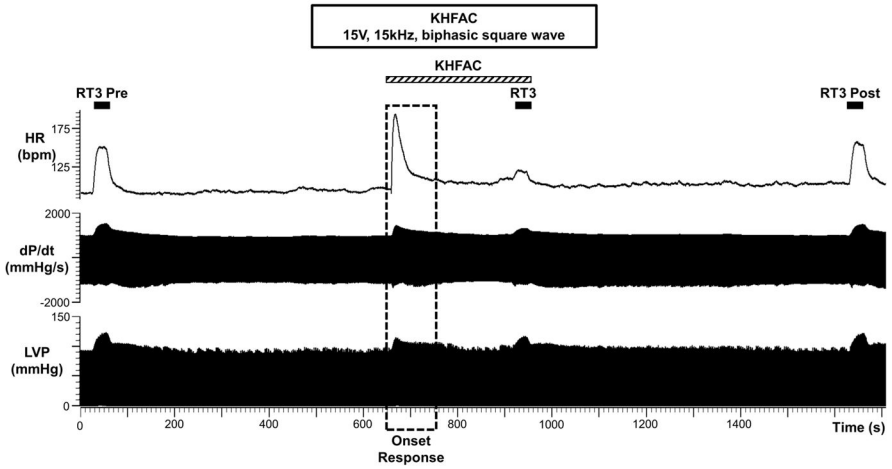

Figure 2.

An example of the cardiac hemodynamic response to paravertebral chain stimulation at the T3 level prior to (pre), during KHFAC (15KHz, 15Volts) and in the recovery phase (post). Shown are induced changes in heart rate (HR), LV dp/dt and LV Pressure (LVP). Note also the cardiac response at KFHAC onset reflective of transient activation of underlying sympathetic axons, the “onset” response. The ~80% block of functional sympathetic control of the heart during KHFAC was readily reversible as indicated the T3 stimulation in the recovery phase (RT3 post).

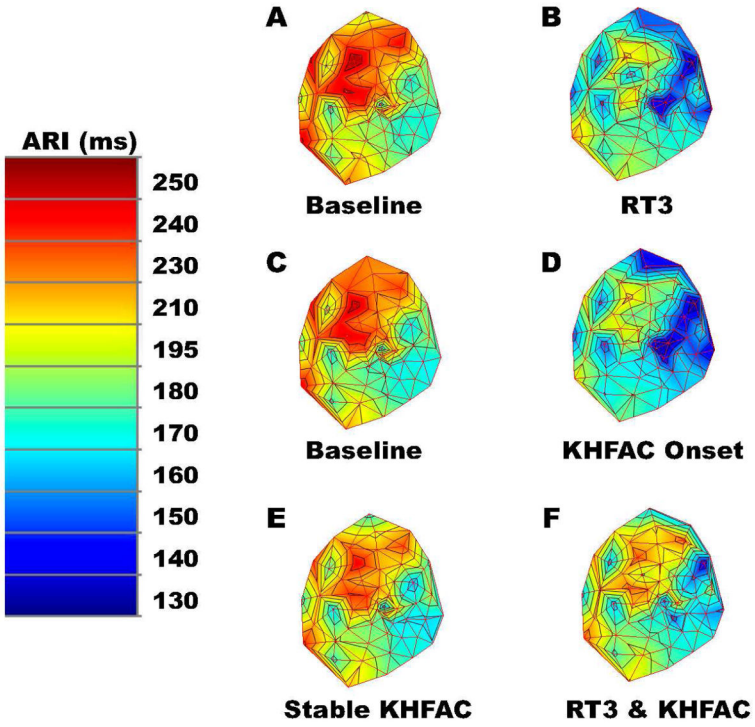

Figure 3.

Representative polar map of ARI (ms) in one animal comparing baseline intact (panels A and C) conditions, with right T3 ganglion stimulation (RT3) (panel B), during the onset (panel D) and stable phase of KHFAC (panel E) and with RT3 applied during the stable phase of KHFAC (panel F). The pattern of ARI shortening was similar between RT3 stimulation and onset of KHFAC as applied to T1–T2 region of paravertebral chain. In the stable phase of KHFAC, ARI returned towards baseline, but remained shortened. KHFAC mitigated the ARI shortening associated with RT3 stimulation.

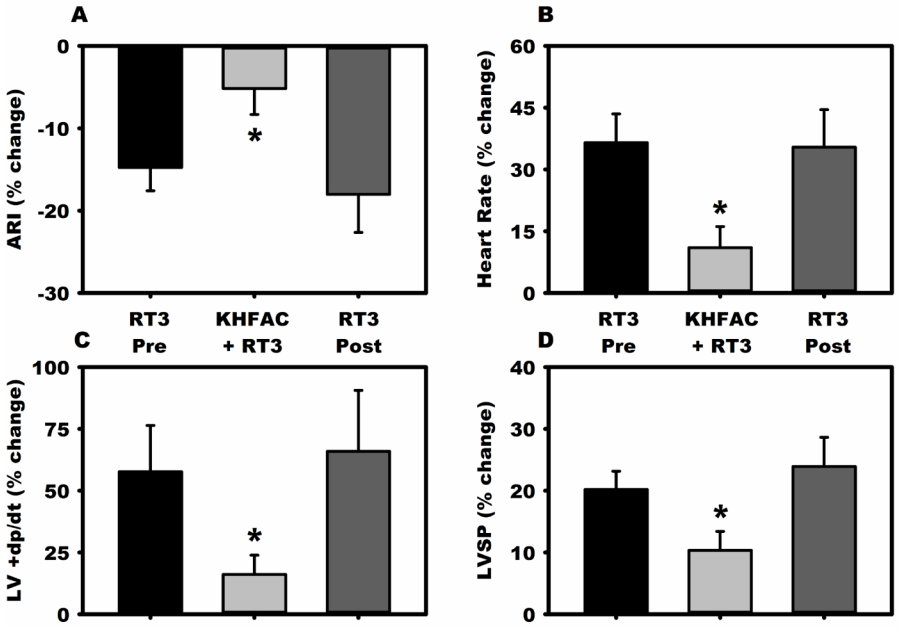

Figure 4.

The percentage change in ventricular ARI (panel A), heart rate (panel B), LV dp/dt (panel C) and LVSP (panel D) in response to T3 stimulation prior to (RT3 pre), during KHFAC (KHFAC+RT3) and in the recovery phase after bioelectronic blockade (RT3 post). * = $p<0.05$

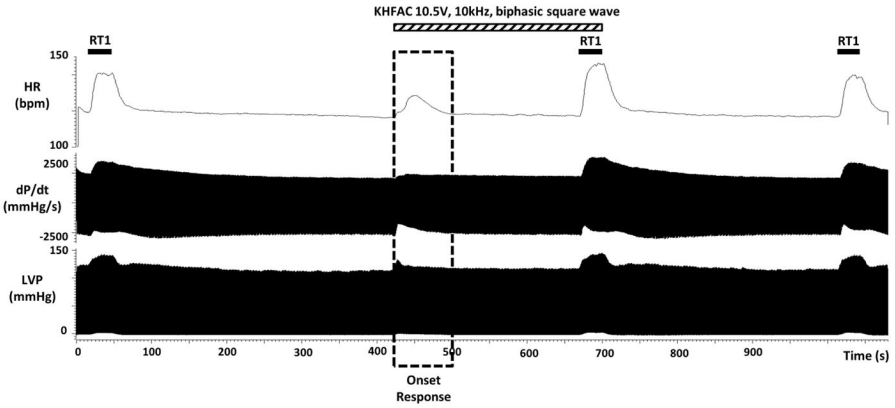

Figure 5.

Response to T1 stimulation prior to and during T1–T2 KHFAC. Note the maintained response in heart rate, LV +dp/dt and LVSP during blocking currents applied caudal to stellate stimulation.

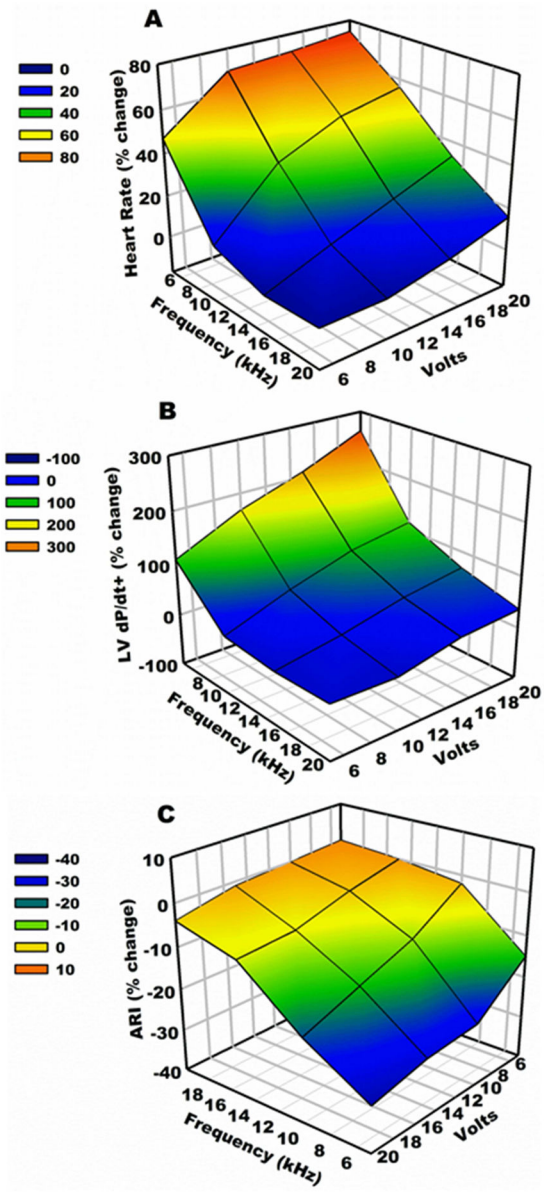

Figure 6.

Effects on KHFAC frequency and intensity on magnitude of the onset response for heart rate (panel A), LV dPdt+ (panel B), and ARI (panel C – note frequency and voltage axis values are reversed relative to panel A and B). Lower frequency and higher voltage resulted in a greater onset response.